Experimental proof of the existence of a weak antiferromagnetic component in yttrium orthoferrite

V. P. Plakhtiĭ, Yu. P. Chernenkov, Zh. Shveitser,* and M. N. Bedrisova

Leningrad Institute of Nuclear Physics, Academy of Sciences of the USSR
(Submitted 24 December 1980)
Zh. Eksp. Teor. Fiz. **80**, 2465–2474 (June 1981)

A new neutron-diffraction technique involving post-scattering-polarization analysis is described. The weak antiferromagnetic component due to the antisymmetric exchange interaction has been detected in yttrium orthoferrite with the aid of the polarization-analysis technique. The experimental value for the magnitude of this component is in good agreement with the theoretical value obtained under the assumption that the Dzyaloshinskiĭ vector is perpendicular to the plane passing through the two interacting magnetic atoms and the intervening oxygen atom.

PACS numbers: 75.30.Et, 75.25. + z

INTRODUCTION

The Dzyaloshinskiĭ–Moriya antisymmetric exchange interaction

$$H_a = \sum_{ij} \mathbf{D}_{ij}[\mathbf{S}_i\mathbf{S}_j] \qquad (1)$$

can give rise to not only weak ferromagnetism, but also weak antiferromagnetism, i.e., a small deviation from collinearity of the antiferromagnetic sublattices without the appearance of a spontaneous moment.[1] The weak antiferromagnetic component practically does not manifest itself in magnetic measurements, and can be detected only by the neutron-diffraction method. But the intensity of the corresponding diffraction peaks, which is proportional to the square of this component, should be very small: usually three-to-four orders of magnitude smaller than the intensity of the reflections due to the base magnitude structure. The difficulty in observing such weak reflections lies in the fact that higher-order and multiple reflections, whose intensities can be 10–100 times higher, are superposed on them. Polarization analysis of the scattered neutrons in principle allows the separation of weak magnetic peaks, but the existing neutron-diffraction technique involving polarization analysis has such a low luminosity that it is practicable only on high-flux reactors. In the present paper we describe a technique possessing a significantly higher luminosity. It has been used to search for a weak antiferromagnetic component in yttrium orthoferrite. The obtained result is discussed in the approximation in which we consider only the indirect exchange interaction between the nearest magnetic ions bound by an intervening anion; in this approximation $\mathbf{D}_{ij}$ has the form of a vector product of the radius vectors of the bonds.

THE DIFFRACTOMETER

In magnetic Bragg scattering, the direction of the neutron spin may be reversed, or may remain unchanged, depending on the orientation of the atomic magnetic moments relative to the neutron-beam-polarization vector $\mathbf{P}_0$ and the scattering vector

$$\boldsymbol{\tau} = \mathbf{k} - \mathbf{k}_0, \quad |\boldsymbol{\tau}| = 2\pi/d, \qquad (2)$$

where k_0 and k are the wave vectors of the scattered neutrons and d is the interplanar spacing. In spin-flip scattering only those components $S_\perp$ of the atomic magnetic moments which are perpendicular to both the scattering and the polarization vectors are effective.[2,3] The nuclear scattering occurs without spin flipping.

To separate the spin-flip and non-spin-flip scattering cross sections, σ_{sf} and σ_{nsf} respectively, the diffractometer should have a polarizer, an analyzer, and a spin-flipping device (a flipper). The polarization efficiency of the apparatus is

$$P_0 = P_p P_a \gamma, \qquad (3)$$

where P_p and P_a are the polarizing powers of the polarizer and the analyzer and γ is the efficiency of the flipper. Since P_0 is always less than unity, σ_{sf} and σ_{nsf} cannot be fully separated, and in measuring, for example, σ_{sf}, we in fact measure

$$\sigma = \sigma_{sf} + \sigma_{nsf}/R_0, \qquad (4)$$

where the polarization ratio

$$R_0 = (1+P_0)/(1-P_0).$$

Nevertheless, at the actually attainable values of $P_0 \sim 0.96$–0.98 the contribution of σ_{nsf} to σ is 50–100 times smaller than the contribution when the polarization analysis is not performed (i.e., when $R_0 = 1$). Thus, it becomes possible to separate out the weak magnetic peaks due to the perpendicular component ($S_\perp$) of the magnetic moment against the background of strong nuclear peaks or magnetic peaks due to the parallel component.

Figure 1a shows a schematic drawing of the usual diffractometer that allows polarization analysis to be carried out.[4] The neutrons are monochromated with the aid of a magnetized crystal whose magnetic structure amplitude is exactly equal to the nuclear structure amplitude, so that the monochromator at the same time performs the function of a polarizer. As the analyzer, a second crystal of the same kind is used. Unfortunately, crystals with a fairly high polarization efficiency have low reflectivities. Thus, the reflection coefficient at the maximum of the 111 diffraction peak of a Heusler-

 0038-5646/81/061291-06$02.40 © 1982 American Institute of Physics

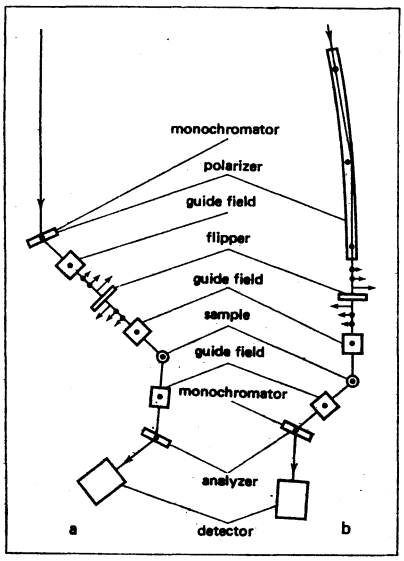

FIG. 1. Schematic diagrams of diffractometers for polarization analysis: a) with two crystals; b) with one crystal and a neutron guide. The arrows indicate the directions of the magnetic fields along the path of the neutrons.

alloy (Cu_2MnAl) crystal is about 6% at a wavelength of 1 Å, which is almost ten times smaller than the corresponding value for the best crystal-monochromators. Therefore, the luminosity of such an instrument is very low: it is approximately an order of magnitude smaller than the luminosity of a polarization-nonanalyzing polarized-neutron diffractometer and two orders of magnitude smaller than that of an unpolarized-neutron diffractometer.

In our diffractometer, one of the crystals was replaced by a high-efficiency polarizing neutron guide[5] with a transmission coefficient close to unity, which led to a significant increase in the luminosity. Figure 1b shows a schematic drawing of the diffractometer. As the polarizer, we use a 5-m neutron guide with an 8-mm-wide window. The sample is located in the white beam, the neutrons being monochromated after the scattering by the sample. A Heusler-alloy crystal performs the functions of a monochromator and an analyzer. The spin flipping is effected with the aid of a nonadiabatic flipper, which is a plane layer of current-carrying conductors.[6] A 96% polarization, which was primarily determined by the polarizing power of the neutron guide, was obtained with a flipper current of 4.5 A (Ref. 5). A wavelength of $\lambda = 2.019$ Å was chosen near the peak of the spectrum at the exit of the neutron guide. The monochromatic neutron flux after the analyzer was then ~10^5 neutrons/cm^2-sec.

Formulas have been derived for the resolution and the luminosity of the neutron diffractometer by Caglioti.[7] They contain as parameters the divergence of the collimators and the mosaic spreads β_1 and β_2 of the crystal monochromator and the sample respectively. These formulas are valid in our case also if the monochromator is mounted after the sample and the following change is made: β_1 is now the mosaic spread of the sample and β_2 is that of the monochromator. It should also be borne in mind that the dispersion parameter $a = \tan\theta_m/\tan\theta$ (θ is the Bragg angle and θ_m is the Bragg angle of the monochromator) decreases with increasing θ, in contrast to the standard scheme, for which $a = \tan\theta/\tan\theta_m$. As usual, the integrated intensity (L) measured in the 2θ-scans does not depend on θ, whereas the integrated ω-scan intensity $R = R(\theta)$. If we take account of the fact that the spectral-line with varies with θ in our case, i.e., that $R_\lambda = R\cot\theta$ (Ref. 8), then from (7) we obtain the relation

$$(L/R_\lambda)^2 = U + V\,\mathrm{tg}\,\theta + W\,\mathrm{tg}^2\theta. \qquad (6)$$

This dependence, with the parameters U, V, and W determined by the method of least squares, was used to obtain the true values of the intensity when the measurements were performed by the ω-scan technique.

CHOICE OF THE OBJECT AND THE EXPERIMENTAL CONDITIONS

Weak antiferromagnetism, like weak ferromagnetism, can be related not only with antisymmetric exchange, but also with uniaxial anisotropy. The stronger the dominant symmetric exchange interaction.

$$H_s = \sum_{ij} J_{ij}\mathbf{S}_i\mathbf{S}_j, \qquad (7)$$

which leads to the establishment of magnetic order, is, the stronger is the antisymmetric interaction. The anisotropy, on the other hand, does not depend on how strong the exchange is. Therefore, it can be expected that the antisymmetric interaction is dominant in crystals with high Néel temperatures.[1] As has been shown,[9,10] it is almost entirely responsible for the weak ferromagnetism in the orthoferrites. Besides the small ferromagnetic moments, the symmetry of the orthoferrites admits of weak antiferromagnetism,[11] which also should largely be due to the antisymmetric exchange.[12]

Crystals of the orthoferrites $RFeO_3$, where R is a rare-earth element or yttrium, have the space group D_{2h}^{16} ($Pbnm$) and a unit cell containing four formula units. For $YFeO_3$, $a = 5.2819(2)$ Å, $b = 5.5957(5)$ Å, $c = 7.6042(4)$ Å (Ref. 13). (Here and below the experimental errors are given in brackets.) The ordering of the spins of the four iron atoms, whose positions in the unit cell are shown in Fig. 2a, is described by the vectors

$$\begin{aligned} &2\mathbf{F} = \mathbf{S}_1 + \mathbf{S}_2 + \mathbf{S}_3 + \mathbf{S}_4, \quad 2\mathbf{G} = \mathbf{S}_1 - \mathbf{S}_2 + \mathbf{S}_3 - \mathbf{S}_4, \\ &2\mathbf{A} = \mathbf{S}_1 - \mathbf{S}_2 - \mathbf{S}_3 + \mathbf{S}_4, \quad 2\mathbf{C} = \mathbf{S}_1 + \mathbf{S}_2 - \mathbf{S}_3 - \mathbf{S}_4. \end{aligned} \qquad (8)$$

The components of the vectors F, G, A, and C belonging to the same irreducible representation Γ_i transform in identical fashion under the action of the symmetry elements of the space group D_{2h}^{16} (Ref. 14). The irreducible representation $\Gamma_4(G_xA_yF_z)$ is realized at fairly high temperatures in the rare-earch orthoferrites and at all $T < T_N$ in yttrium orthoferrite. The base antiferromagnetic component G_x is directed along the a axis; the weak ferromagnetic moment F_z, along the c axis; and the weak antiferromagnetic component A_y, if it exists, should be directed along the b axis. The proposed magnetic structure (a "cross" type of structure) is shown in Fig. 2b.

The components G, A, and F correspond to different

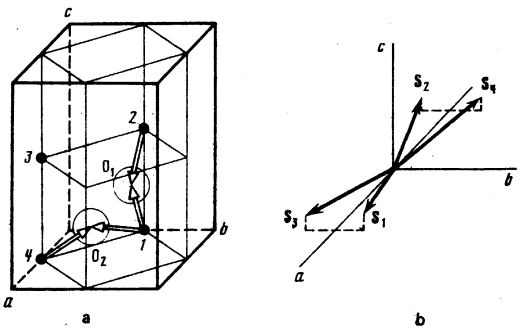

FIG. 2. a) Unit cell of an orthoferrite. The four Fe^{3+} ions and the oxygen ions effecting the bond between the nearest neighbors are indicated. b) The ordering of the Fe^{3+} spins, according to Ref. 11.

nonoverlapping systems of magnetic diffraction peaks:

$h+k=2n+1$; $l=2n+1$ for G,

$h+k=2n$; $l=2n+1$ for A,

$h+k=2n$; $l=2n$ for F.

Since the intensity of the A peaks should be very low, it is first of all necessary that the strong peaks of nuclear nature be not superposed on them. This condition is fulfilled for reflections of the $00l$ ($l=2n+1$) and $h0l$ ($h+l=2n+1$) types, since they are forbidden by the extinction law.[15] Such reflections can be due only to the weak antiferromagnetic component A_y.

A $YFeO_3$ crystal in the form of an octahedral prism of height 5 mm and with transverse dimensions ~4 mm was mounted on a goniometric head in a ~0.1-T field produced by a permanent magnet. (According to Umebayachi and Isikawa,[16] saturation sets in at $H<0.01$ T when the field is applied along the weak-ferromagnetism c-axis.) We measured four reflections of the A type: the 201 reflection in a vertical field and the 001, 003, and 005 reflections in a horizontal field on the sample. In both cases the weak-antiferromagnetism vector A was perpendicular to the scattering vector τ and the external magnetic field H, whose direction coincided to within ~2° with that of the field inside the crystal. The measurement of the polarization acquired in the nuclear reflections showed that a depolarization of the beam could not have occurred as a result of nonadiabatic transitions at the crystal boundaries, or as a result of the incomplete saturation of the crystal.

ELIMINATION OF MULTIPLE SCATTERING

When one of the crystal planes (HKL) is set in the reflecting position (Fig. 3), it may turn out that the Bragg condition is fulfilled also for some other plane (hkl). Even if the HKL reflection is forbidden by symmetry, there will be observed at the corresponding Bragg angle (2θ) a diffraction peak due to double reflections: from first the (hkl) and then the ($H-h, K-k, L-l$) planes provided these two reflections are allowed. The most intense double spin-flip processes will occur in those cases in which either the first or second reflection is caused by the base magnetic structure G_x ($h+k=2n+1$; $l=2n+1$ or $H-h+K-k=2n+1$; $L-l=2n+1$). If the first or the second reflection is connected with F_x or

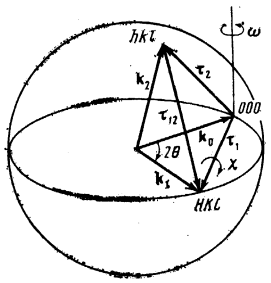

FIG. 3. Vector diagram of double scattering.

A_y, spin-flip scattering can also occur, but the cross section for such processes is much smaller. Finally, because of the incomplete polarization of the neutron beam, a small contribution to the spin-flip scattering may be made by the double processes in which both reflections are nuclear reflections.

In order to eliminate the double reflections without violating the Bragg condition for (HKL), we must rotate the crystal about the scattering vector τ_1 (the angle χ) until the parasitic (hkl) site leaves the Ewald sphere (Fig. 3). But because of the finite resolution, the double scattering can be fairly intense even when the Bragg condition is not entirely fulfilled for (hkl). Therefore, in measuring each A-type reflection, we chose that value of the angle χ for which the distance from the Ewald sphere to the nearest parasitic site was maximal. The contribution $I_{12}(\omega_1, \chi)$ of the double scattering to the peak intensity $I_1(\omega_1)$ of the A reflection was computed in the crudest approximation, i.e., in the approximation in which $\Delta_1=\Delta_2=\Delta$ for all the reciprocal-lattice sites (Δ_1 and Δ_2 are respectively the widths of the HKL and hkl reflections in the ω-scan). The structure factors were computed from the general formula (12)

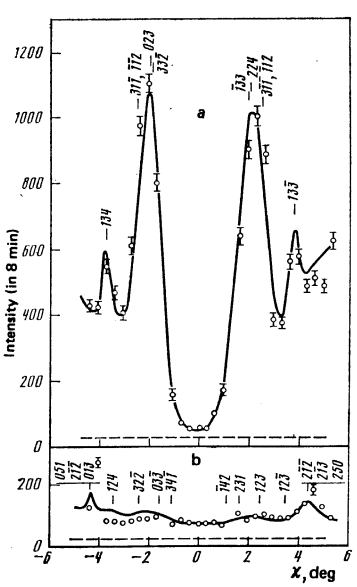

FIG. 4. Variation of the peak intensity of the 201 reflection as the crystal is rotated about the scattering vector in the case of: a) non-spin-flip scattering; b) spin-flip scattering. The solid curve is the computed curve; the dashed line represents the background-noise level. The positions and indices of the parasitic sites participating in the double scattering are indicated.

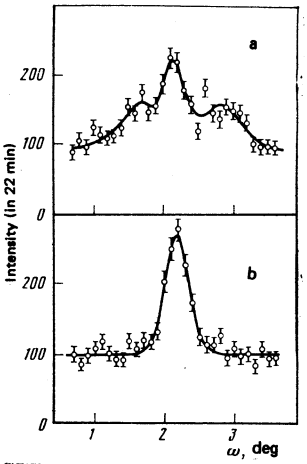

FIG. 5. Profile of the 201 reflection in the ω-scan procedure ($\chi = 0°$) in the case of: a) non-spin-flip scattering; b) spin-flip scattering.

of Ref. 4 with allowance for the incomplete polarization. In Fig. 4 we show together with experimental points the computed curve for the peak intensity of the 201 reflection

$$I(\omega_1, \chi) = I_{12}(\omega_1, \chi) + I_1(\omega_1) + I_b, \tag{9}$$

where I_b is the background intensity. For $\chi = 0°$ (the b axis lies in the scattering plane) the intensity of the double spin-flip scattering is negligibly small, as compared to the intensity of the χ-independent single scattering. The profile $I(\omega, 0)$ of the 201 reflection is shown in Fig. 5. In the case of spin-flip scattering the peak has the Gaussian form, which is characteristic of single reflection, whereas secondary peaks due to double processes involving the nearest parasitic sites are observed in non-spin-flip scattering.

ALLOWANCE FOR THE HIGHER ORDERS

If the neutrons are monochromatized with the aid of a crystal, then the spectrum contains, besides the principal line with wavelength λ, higher-order harmonics (λ/n) that give nH, nK, and nL reflections superposed on the measured HKL reflection. In the orthoferrites the even orders, which coincide with the A-type reflections, have a primarily nuclear character. (The weak-ferromagnetism-related-magnetic-scattering admixture is insignificant.) The odd higher-order reflections are, like the first-order reflection, due to weak antiferromagnetism, and therefore their intensity will be negligibly small.

The spectrum, measured by the time-of-flight method, at the exit of the neutron guide used in the present investigation is given in Ref. 5. The ratio of the ($\lambda/2$)- and λ-neutron fluxes is equal to 4×10^{-2}; the actual value should be somewhat lower, since the short-wave part of the time-of-flight spectrum is drawn out because of poor resolution. Owing to the fact that the transmission of the neutron guide falls sharply with decreasing wavelength, we need to worry about how to decrease the contribution of only the second harmonic. Unfortunately, the polarizing power of a Cu_2MnAl crystal for the 222 reflection is not high, still the polarization analysis decreases the intensity of the second-order parasitic reflections by a considerable factor. If, moreover, we take account of the fact that the reflectivities of the monochromator and the sample decrease somewhat with decreasing wavelength, then we can expect the second-order reflections to be comparable in intensity to the A-type reflections.

The contribution of the second harmonic to the spin-flip scattering was determined with the aid of a filter based on samarium, which has a resonance at $\lambda = 0.92$ Å. The filter was prepared from a mixture of Sm_2O_3 and Al powders. The attenuation factor was 6 for λ and, according to Hughes *et al.*,[17] 19 for $\lambda/2$. Using this filter, we measured the intensities of the second-order 020 and 402 reflections, which coincide in position with the first-order 010 and 201 reflections, the first of which is forbidden by symmetry and the second is due to weak antiferromagnetism. A comparison of these intensities with the computed values yielded $I_{\lambda/2}/I_\lambda = 5(1) \times 10^{-3}$. The contribution of the second orders to the measured A-type reflections was then 20–80%.

DETERMINATION OF THE QUANTITY A_y

The magnitude of the weak antiferromagnetic component can be determined by comparing the intensities of the A- and G-type reflections in the spherically-symmetric form-factor approximation,[18] which is sufficient for the accuracy with which the intensities of the A reflections were measured. (In the best case the relative error was 16%.) The problem is, however, complicated by the fact that in computing the true G-reflection intensities we must take account of the extinction, which is insignificant for the weak A reflections. For the nuclear and G reflections, extinction was certainly strong, firstly, because of the relatively large crystal dimensions, which ensured an appreciable A-reflection intensity and, secondly, because of the long wavelength of the neutrons. In the present case the wavelength was determined by the parameters of the neutron guide, but its decrease was in principle undesirable, since this would have resulted in an increase in the probability for multiple scattering.

The integrated intensity of the diffraction peaks was computed with allowance for the primary and secondary extinctions, using the formulas[19]

$$I = kQ(1+2\varepsilon Q)^{-1/2}, \quad Q = \lambda^3 F^2 / V_c^2 \sin 2\theta,$$
$$\varepsilon = 2\frac{t^2 \sin 2\theta}{3\lambda} + T\left[\frac{1}{2}\left(\frac{10^{-4}\lambda}{t \sin 2\theta}\right)^2 + \pi\eta^2\right]^{-1/2}, \tag{10}$$

where k is a proportionality factor, F is the structure amplitude, V_c is the volume of the unit cell, T is the mean dimension of the crystal, t is the mean dimension of the mosaic blocks, and η is the misorientation of the blocks (the mosaic spread). The parameters t and η, which determine the magnitude of the extinction correction ε, where obtained by the method of least squares from the intensities of 27 reflections measured with unpolarized neutrons with $\lambda = 1.102$ Å. We computed the structure amplitudes with the atomic coordinates and thermal factors obtained in Ref. 11. We varied the parameters k, t, and η, as well as the mag-

netic amplitude a_m of the Fe^{3+} ion. The intensities computed with $t=19$ and $\eta=1.5\times10^{-4}$ rad are in fairly good agreement with the measured intensities (convergence factor $R=0.07$). The formulas used remain valid when $\lambda=2.019$ Å, although the extinction correction becomes very large. In this case a fairly good agreement with experiment ($R=0.10$) was achieved for 16 reflections (including five G-type magnetic reflections: 011, 013, 031, 033, and 015) with the same t and η values by varying the proportionality factor and the magnetic amplitude. Having thus obtained k and a_m, we could compute from the measured intensities of the A-type reflections the ratio $A_y/G_x=1.93(18)\times10^{-2}$.

DISCUSSION

Keffer[20] has phenomenologically proposed for a pair of magnetic ions bound by an intervening anion a Dzyaloshinskiĭ vector in the form $\mathbf{D}_{ij}\sim\mathbf{r}_{i0}\mathbf{r}_{j0}$ in terms of the radius vectors $\mathbf{r}_{i0}$ and $\mathbf{r}_{j0}$ of the bonds. An analysis of the generalized Hamiltonian for the indirect exchange interaction in such a system[21] has shown that

$$\mathbf{D}_{ij}=\mathscr{D}[\mathbf{r}_{i0}\mathbf{r}_{j0}];\quad \mathscr{D}=d_1+d_2\cos\theta, \tag{11}$$

where d_1 and d_2 are some constants and θ is the bond angle. In the orthoferrites the nearest Fe^{3+} ions are bound by oxygen ions. The relation (11) allows us to express the components of the Dzyaloshinskiĭ vectors $\mathbf{D}_{ij}$ in terms of the coordinates of the oxygen ions [O_1: x_1, y_1, z_1 and O_2: x_2, y_2, z_2 (Fig. 2a)], the bond lengths l_1 and l_2, and the unit-cell parameters a, b, and c.[12] If we neglect the small differences in the lengths and angles of the various bonds, then for the two nearest Fe^{3+} ions located along the c axis

$$D_{12}^x=\mathscr{D}\frac{bc}{2l^2}\left(\frac{1}{2}-y_1\right),\quad D_{12}^y=\mathscr{D}\frac{ac}{2l^2}x_1,\quad D_{12}^z=0. \tag{12}$$

For the remaining four ions lying in the basal plane we have

$$D_{14}^x=\mathscr{D}\frac{bc}{2l^2}z_2,\quad D_{14}^y=\mathscr{D}\frac{ac}{2l^2}z_2,\quad D_{14}^z=\mathscr{D}\frac{ab}{2l^2}\left(x_2-y_2-\frac{1}{2}\right) \tag{13}$$

In the nearest-neighbor approximation, and with only the symmetric and antisymmetric exchange interactions, (7) and (1) respectively, taken into account, the free energy has up to terms of second order in smallness the form[12,22]

$$\begin{aligned}\Phi=&3J\mathbf{F}^2-3J\mathbf{G}^2+J\mathbf{A}^2-J\mathbf{C}^2+2D_{12}^x(G_yC_z-G_zC_y)\\&+(4D_{14}^y+2D_{12}^y)(G_zF_x-G_xF_z)+4D_{14}^z(G_xA_y-G_yA_x).\end{aligned} \tag{14}$$

From this we have for the $\Gamma_4(G_xA_yF_z)$ configuration the relations[1)]

$$F_z=\frac{2D_{14}^y+D_{12}^y}{3J}G_x,\quad A_y=-\frac{2D_{14}^z}{J}G_x. \tag{15}$$

Knowing the structure parameters and the experimental value for F_z/G_x, we can compute A_y/G_x. The structure of $YFeO_3$ has been determined with a high accuracy by Coppens and Eibschütz.[13] As for the small ferromagnetic moment, there are some discrepancies among the values given in different papers. According to the data of Judin *et al.*,[23] $F_z/G_x=0.9\times10^{-2}$. Treves *et al.*[10,24] obtained the values 0.89×10^{-2} and 1.2×10^{-2} in their investigations, while Jacobs *et al.*[25] obtained the value 1.08×10^{-2}. It is reasonable to choose the minimum of these values, since the possible ferromagnetic impurities, even in very small amounts, can lead to a situation in which the spontaneous moment determined from magnetic measurements will be greatly overestimated. The thus computed ratio $A_y/G_x=1.95\times10^{-2}$ coincides with the experimental value obtained by us.

We computed A_y/G_x with the theoretical value of A_y/F_z (=2.19), which, as has been noted before,[12] depends little on the form of $\mathscr{D}$, and is largely determined by the vector product $[\mathbf{r}_{j0}\times\mathbf{r}_{j0}]$. The agreement between the experimental and computed values for A_y/G_x indicate that the Dzyaloshinskiĭ vector is perpendicular to the plane passing through the Fe–O–Fe bond. In this case the formulas (12), (13), and (15) allow us to compute $\mathscr{D}$, the components of the vectors $\mathbf{D}_{12}$ and $\mathbf{D}_{14}$, and their lengths from the experimental A_y/G_x value. In units of $J\times10^{-2}$, we have $\mathscr{D}=2.31(22)$; $D_{12}^x=0.48(4)$; $D_{12}^y=1.30(12)$; $D_{12}^z=0$; $D_{14}^x=0.72(7)$; $D_{14}^y=0.55(5)$; $D_{14}^z=-0.96(9)$; $|\mathbf{D}_{12}|=|\mathbf{D}_{14}|=1.35(13)$.

In conclusion, we express our gratitude to V.A. Priemyshev, Ya.A. Kasman, S.M. Rusin, K.I. Turapina, and L.P. Kolesnikova, who participated in the construction of the diffractometer, R.V. Pisarev, who kindly made the yttrium orthoferrite crystal available to us, and V.M. Lobashev for the opportunity to perform the experiment with the polarizing neutron guide.

*) Center for Nuclear Research, Grenoble, France.

1) The expression given in Ref. 12 for A_y is incorrect.

[1] T. Moriya, Phys. Rev. **120**, 91 (1960).
[2] Yu. A. Izyumov and S. V. Maleev, Zh. Eksp. Teor. Fiz. **41**, 1644 (1961) [Sov. Phys. JETP **14**, 1168 (1962)].
[3] M. Blume, Phys. Rev. **130**, 1670 (1963).
[4] P. M. Moon, T. Riste, and W. C. Koehler, Phys. Rev. **181**, 920 (1969).
[5] A. P. Bulkin, B. Ya. Kezerashvili, V. A. Kudryashev, A. N. Pirozhkov, V. G. Syromyatnikov, V. P. Kharchenkov, and A. F. Shchebetov, Preprint Leningradskiĭ Inst. Yad. Fiz., 505, Leningrad, 1979.
[6] K. Abrahams, O. Steinsvoll, P. J. Bongaarts, and P. W. de Lange, Rev. Sci. Instrum. **33**, 524 (1962).
[7] G. Caglioti, Acta Crystallogr. **17**, 1202 (1964).
[8] G. E. Bacon, Neutron Diffraction, Clarendon Press, Oxford, 1975.
[9] D. Treves, Phys. Rev. **125**, 1843 (1962).
[10] D. Treves, J. Appl. Phys. **36**, 1093 (1965).
[11] E. A. Turov and V. E. Najs, J. Met. (USSR) **9**, 10 (1960); **11**, 161 (1961).
[12] A. S. Moskvin and E. V. Sinitsyn, Fiz. Tverd. Tela (Leningrad) **17**, 2495 [Sov. Phys. Solid State **17**, 1664 (1975)].
[13] P. Coppens and M. Eibschütz, Acta Crystallogr. **19**, 524 (1965).
[14] E. F. Bertaut, in: Magnetism, Vol. III (Ed. G. T. Rado and H. Suhl), Academic Press, New York, 1963, p. 149.
[15] International Tables for X-Ray Crystallography, Kynoch Press, Birmingham, 1965.
[16] H. Umebayachi and Y. Isikava, J. Phys. Soc. Jpn. **20**, 2193 (1965).
[17] D. J. Hughes, B. A. Mgurno, and M. K. Brussel, Neutron Cross Sections, BNL 325, 2nd ed., 1960.
[18] R. E. Watson and A. J. Freeman, Acta Crystallogr. **14**, 27 (1961).
[19] P. J. Becker and P. Coppens, Acta Crystallogr. Sect. A **30**,

129 (1974).
[20]F. Keffer, Phys. Rev. **126**, 896 (1962).
[21]A. S. Moskvin and E. V. Sinitsyn, Fiz. Tverd. Tela (Leningrad) **14**, 2535 (1972) [Sov. Phys. Solid State **14**, 2198 (1973)].
[22]T. Yamaguchi, J. Phys. Chem. Solids **35**, 479 (1974).
[23]V. M. Judin, A. B. Sherman, and I. E. Mylnikova, Phys. Lett. **22**, 554 (1966).
[24]G. Gorodetsky, S. Strikman, Y. Tenenbaum, and D. Treves, Phys. Rev. **181**, 823 (1969).
[25]I. S. Jacobs, H. F. Burne, and L. M. Levinson, J. Appl. Phys. **42**, 1631 (1971).

Translated by A. K. Agyei